INTERNATIONAL JOURNAL OF AUTOMOTIVE AND MECHANICAL ENGINEERING
ISSN: 2229-8649 e-ISSN: 2180-1606
VOLUME 22, ISSUE 4, 2025, 13058 - 13069
DOI: https://doi.org/10.15282/ijame.22.4.2025.17.0994

RESEARCH ARTICLE

Effect of Windbreakers on the Aerodynamic Performance of a High-Speed Train Using CFD Analysis

N. A. Norhelmi[1], I. A. Ishak[1]*, M. Arafat[1], N. M. Maruai[2], N. H. Shaharuddin[3], N. A. Samiran[4], N. Darlis[1], R. A. Jalil[5]

[1]Faculty of Engineering Technology, Universiti Tun Hussein Onn Malaysia, Education Hub, Pagoh, 84600, Johor

[2]Department of Mechanical Precision Engineering, Malaysia-Japan International Institute of Technology, Universiti Teknologi Malaysia, Jalan Sultan Yahya Petra, 54100, Kuala Lumpur, Malaysia

[3]Department of Mechanical Engineering, Keio University, Yokohama, Japan

[4]Faculty of Mechanical Engineering, Universiti Tun Hussein Onn Malaysia, Persiaran Tun Dr. Ismail, 86400 Parit Raja, Johor

[5]K.L. Consult Associates Sdn Bhd, Unit 158-4-5, Kompleks Maluri, Jalan Jejaka, Taman Maluri, Cheras, 55100 Kuala Lumpur, Malaysia

ABSTRACT – High-speed trains are designed to reduce air resistance, lower noise levels, and ensure stable, smooth travel. Windbreakers, which serve to reduce side forces caused by crosswinds, are essential for maintaining the stability and safety of high-speed trains, especially at high speeds. This study investigates the effects of windbreaker height and porosity on the aerodynamics of a high-speed train under 30° and 60° crosswind conditions. The windbreakers tested have heights of 65 mm, 135 mm, and 190 mm, with porosities varying in hole sizes of 12.5 mm, 25 mm, and 50 mm, resulting in nine windbreaker designs. Simulations were conducted at 80 m/s to measure drag, side, and lift force coefficients, and to analyze flow structure and pressure contours. The results show that the best aerodynamic performance occurs under 30° crosswind conditions, with the optimal windbreaker design being the tallest height and smallest porosity. Specifically, the drag coefficient (C_d) reached 0.0101, and the side and lift force coefficients (C_s and C_l) were 0.3383 and 0.3290, respectively. The study concludes that optimizing windbreaker height and porosity significantly improves aerodynamic performance, with medium porosity offering the best overall results. However, windbreaker height must be carefully considered under varying crosswind conditions to achieve optimal performance.

ARTICLE HISTORY

Received	:	28th July 2024
Revised	:	15th May 2025
Accepted	:	16th Nov. 2025
Published	:	05th Dec. 2025

KEYWORDS

Crosswind
Aerodynamics
Flow structure
CFD
High-speed train
Windbreakers

1. INTRODUCTION

High-speed trains offer rapid, effective, and easy long-distance travel choices, marking a substantial improvement in the transportation sector. Crosswinds, however, pose a serious threat to the stability and safety of these trains, making them one of their most significant obstacles [1], [2]. The lateral forces experienced by high-speed trains in crosswinds can cause instability, raising the possibility of collisions and requiring more regular maintenance because of the increased wear and tear on the components [3]. Several strategies are used to lessen these negative consequences, such as using windbreakers. The mitigation of crosswind-induced aerodynamic loads on high-speed trains is a significant area of research, particularly considering the safety implications of strong winds. Among the various countermeasures explored, windbreakers, whether natural, like vegetation, or engineered, such as solid barriers or mesh fences, have emerged as cost-effective and practical solutions to enhance train stability. Windbreakers are designed to modify local wind flow patterns and reduce lateral wind forces acting on trains, which can mitigate the risk of derailment and improve overall operational safety [4], [5]. They can be positioned strategically along the train's route and can be man-made, like man-made barriers, or natural, like embankments [6], [7]. By disrupting the momentum of approaching winds and reshaping the velocity profile, windbreakers reduce lateral wind loading and enhance overall train stability.

However, the aerodynamic performance of windbreakers is highly dependent on design parameters such as height, porosity, geometry, and spacing, as well as their interaction with complex terrain and wind conditions [8]. Crosswinds can be effectively blocked by solid concrete walls, which also greatly reduce aerodynamic drag on the train and increase stability and fuel efficiency [9]. In addition to offering modest drag reduction, vegetative windbreaks offer additional ecological benefits and moderate aerodynamic protection; however, their effectiveness is highly sensitive to plant density and maturity [10]. Perforated or mesh fences enable partial flow-through, offering reduced pressure differentials and improved flow reattachment downstream features, which can lead to favorable drag characteristics under specific wind conditions [11]. By lowering wind speed and permitting controlled airflow, hybrid windbreakers, which include solid and porous elements, optimize aerodynamic efficiency, resulting in a balanced reduction in side force coefficient and enhanced train performance.

The effectiveness of windbreakers in mitigating the crosswind effects depends on their design and configuration. Studies have investigated the impact of various parameters, such as the height, length, and orientation of the windbreakers, on the aerodynamic performance of high-speed trains [12], [13]. For example, it has been found that increasing the height

***CORRESPONDING AUTHOR | I. A. Ishak** | ✉ izuan@uthm.edu.my

of the windbreakers can improve the wind-protection performance on both the train and the catenary system [12]. In addition, Researchers have explored the use of different windbreaker designs, such as inclined barriers [14], and windbreakers with buffer equipment [8], to optimize the aerodynamic performance. The literature suggests that the use of properly designed windbreakers can be an effective strategy to mitigate the adverse effects of crosswinds on high-speed trains, thereby improving their safety and stability during operation [8], [15], [16]. While these studies have provided foundational insights, critical gaps remain. A significant portion of the literature has focused on idealized or isolated configurations without exploring how performance varies across different vertical sections of the train. In particular, the altitude-dependent effectiveness of windbreakers, i.e., how performance varies from ground level to rooftop height, has received limited attention. Moreover, the influence of porosity levels on pressure gradients, flow detachment, and recirculation zones has yet to be systematically quantified across realistic crosswind scenarios. Most importantly, while computational fluid dynamics (CFD) has advanced rapidly as a tool for modelling these interactions, few studies present thorough validation of CFD findings against empirical or standardized benchmarks, raising concerns about the generalizability of the results.

Furthermore, the coupling between design parameters (e.g., porosity and height) and aerodynamic metrics (e.g., side force coefficient, lift coefficient, and flow separation patterns) remains poorly understood in multi-variable contexts. In many cases, windbreaker performance is evaluated in terms of gross lateral force reduction, without fully analyzing the trade-offs between different design strategies, such as the possible decrease in effectiveness at mid-height zones when porosity is increased. Therefore, this study aims to bridge this gap by systematically investigating the effects of various windbreaker configurations on the aerodynamic performance of high-speed trains under different crosswind conditions. By conducting comprehensive CFD simulations, this research will provide valuable insights into the optimal placement and design of windbreakers to minimize aerodynamic drag, reduce lateral forces, and enhance overall train stability.

2. METHODS AND MATERIALS

2.1 Geometry Modelling

The first step in the CFD analysis is the geometry modelling of the high-speed train and windbreakers. A generic high-speed train model, designed at a 1/25th scale to optimize computational resources, was selected for the study [17], [18]. The scaled-down model replicates key aerodynamic features of a full-sized train while reducing simulation time and computational demands. The train geometry includes detailed dimensions (Figure 1) to ensure an accurate representation of the flow interaction.

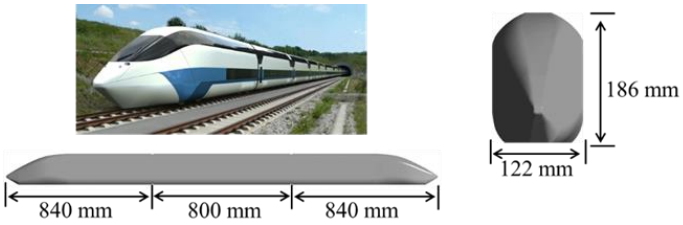

Figure 1. Detailed dimensions of the selected train model at 1/25th scale [18]

Windbreakers of varying heights and porosities were added alongside the train to analyze their impact on the aerodynamic performance under different crosswind conditions, as shown in Figure 2.

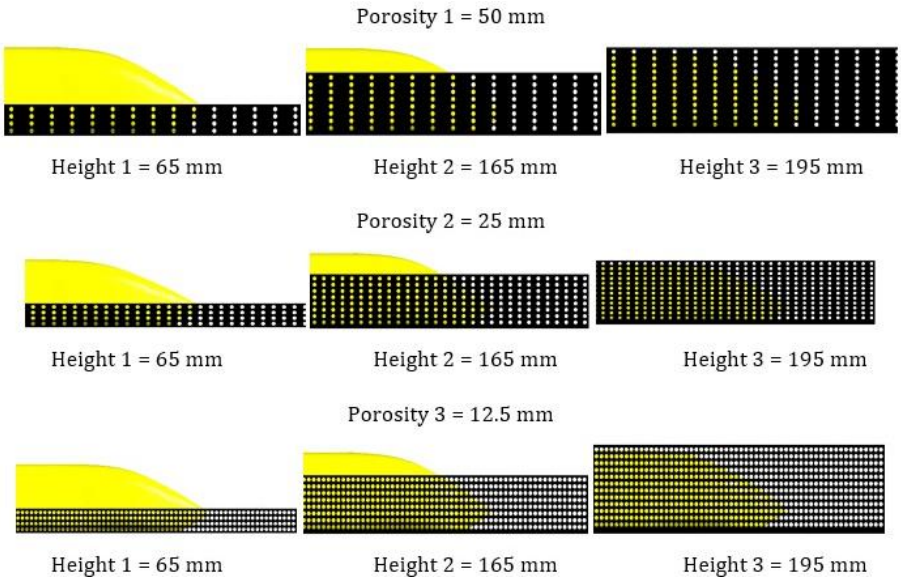

Figure 2. Setup configuration of windbreakers used in the simulation case

These configurations allow for comparisons of the flow structure and aerodynamic loads. These windbreakers were strategically placed near the train to simulate real-world scenarios where windbreakers are installed to mitigate crosswind effects on trains. The train body and windbreakers were positioned within a computational domain large enough to capture relevant flow structures and interactions accurately.

2.2 Simulation Setup and Boundary Conditions

The computational domain, or mesh enclosure, defines the space in which the fluid flow simulation is conducted. Proper enclosure design ensures accurate capture of flow structures and minimizes the influence of boundary conditions on the simulation results. The enclosure was designed to be sufficiently large to avoid artificial interference with flow patterns. Figure 3 illustrates the enclosure size and boundary conditions used in the simulations. The train and windbreakers are centrally positioned within the enclosure to allow airflow to develop naturally before interacting with these structures.

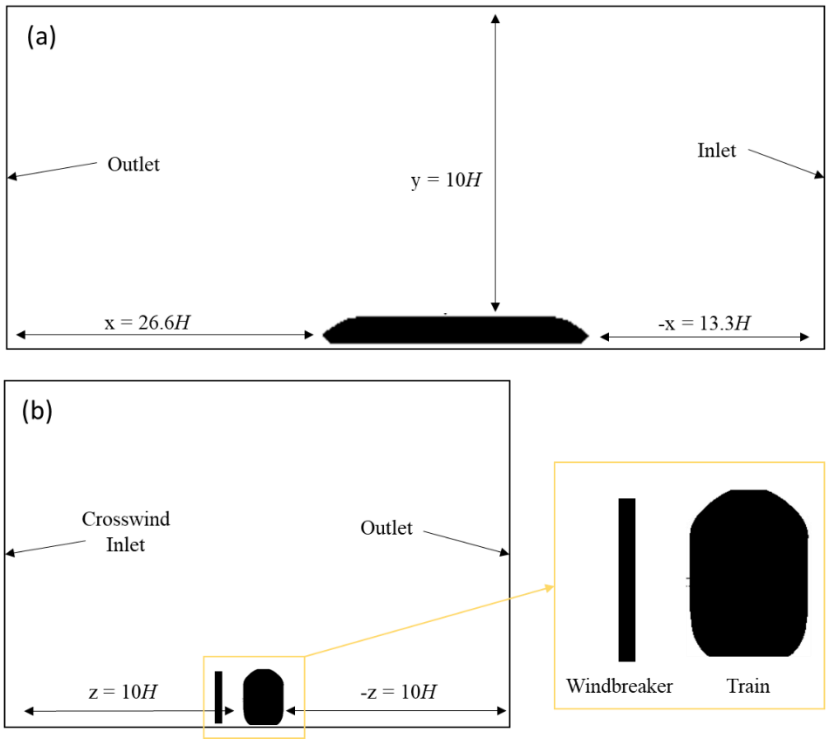

Figure 3. Computational domain and boundary conditions used in the current study

To ensure accurate CFD simulation results, appropriate boundary conditions are essential. A velocity inlet boundary condition was applied at the upstream and left wall to represent the incoming airflow mimicking typical high-speed train operations and crosswind scenarios, with a resultant velocity of 80 m/s. A pressure outlet boundary condition was set at the downstream and wall at the leeward side of the train with a static pressure of 0 Pa, allowing the flow to exit the domain naturally without artificial reflections [19]. Symmetry boundary conditions were implemented on the roof of the domain to reduce computational effort while maintaining accurate flow behavior, assuming symmetric flow conditions [20]. The ground was modeled as a stationary wall with a no-slip condition, accurately simulating the frictional interaction between the ground and airflow [21]. The train body was also modeled as a solid wall with a no-slip condition, ensuring that the fluid velocity at the train surface matches the surface velocity, capturing the effects of viscous flow. Finally, windbreakers were modeled as solid structures with various heights and porosities to analyze their effectiveness in mitigating aerodynamic loads and flow disturbances caused by crosswinds.

The k-omega SST turbulence model was employed to simulate the turbulent flow around the high-speed train. This model is well-suited for this application due to its ability to accurately capture both viscous and freestream effects, particularly in the presence of adverse pressure gradients and near-wall regions [22].

2.3 Grid Independence Study

In Computational Fluid Dynamics (CFD), ensuring the accuracy, reliability, and effectiveness of simulation outcomes is crucial. One method employed to achieve this is the Grid Independence Study. This study aims to determine the ideal mesh size for a simulation, ensuring that as the mesh is refined, the simulation results remain consistent, indicating that the solution has become independent of the grid resolution [23], [24]. The process involves gradually increasing the mesh size until no significant performance improvement can be observed due to the larger mesh size [25]. An unstructured polyhedral-type mesh was selected in the current study. This type of research helps to identify the level of mesh refinement required for a reliable and accurate simulation. Table 1 shows the parameters that have been set up for the meshing for the simulation. The result obtained shows that the percentage difference in the drag coefficient (C_d) shows a converging

pattern towards mesh 4 grid resolution (Figure 4). If the grid resolution increases, the result will be more refined and will not affect the simulation result. Mesh 3 shows a smaller percentage difference (0.46%) than the finest mesh. So, for further study, mesh 3 grid resolution will be used as the setup, as the provided result will be close to the expected result, and the grid is finer. In addition, the aerodynamic force and coefficients were directly calculated using Ansys Fluent user interface based on projected surface area, wind velocity and fluid properties.

Table 1. Parameters used for the grid independence study

Mesh type	Coarse	Medium	Fine	Finest
	Mesh 1	Mesh 2	Mesh 3	Mesh 4
Element Size (mm)	437	218	109	55
Face Sizing (mm)	437	218	109	55
Element number(cells)	57528	249597	323292	452140
Nodes	111061	1253488	1646528	2338170
Drag Coefficient (C_d)	0.2257	0.2220	0.2199	0.2189
Percentage difference (%)		1.67	0.94	0.46

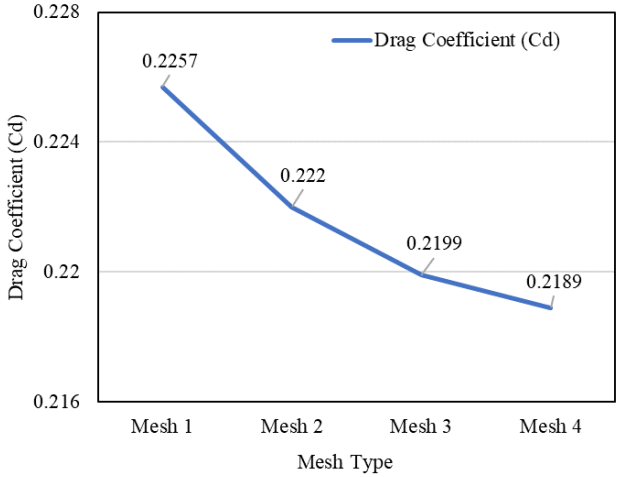

Figure 4. Drag coefficient value for different mesh resolutions

2.4 Validation

To ensure the accuracy of our current simulation, we compared the results with experimental data of the drag coefficient from available research [26]. Notably, the present study demonstrates a reasonable agreement between the simulated aerodynamic drag coefficient and available experimental and numerical benchmarks. The drag coefficient obtained from our selected mesh simulation is 0.22, while the experimental measurement reported in the reference study is 0.18. Additionally, simulations conducted using OpenFOAM yielded a drag coefficient of 0.21, and a related numerical study by Arafat et al. [17] reported a value of 0.19. The relative percentage discrepancy between our CFD result and the experimental data is approximately 22.2%, which is within the expected range for external flow simulations over complex geometries, considering uncertainties in both experimental conditions and computational modeling.

3. RESULTS AND DISCUSSION

The results were categorized into two main groups for analysis: the qualitative group included velocity streamlines and pressure contour formations caused by changes in velocity acting on the train body, and the quantitative group included the drag force coefficient, side force coefficient and lift coefficient.

3.1 Drag Force Coefficient at 30º Crosswind

The drag coefficient (C_d) in a 30º crosswind analysis shows that the performance of windbreakers varies greatly with varying heights and porosities, as shown in Figure 5. Due to interactions with the train's structure, high porosity windbreakers (50 mm) typically have low drag across all heights, peaking slightly at 130 mm. By successfully balancing airflow and wind deflection, medium porosity windbreakers (25 mm) achieve the lowest drag at the highest height, with a decreasing C_d with increasing height. Due to aerodynamic disturbances, low porosity windbreakers (12.5 mm) have the largest drag at mid-height; but, by successfully redirecting the crosswind, they achieve much lower drag at the shortest and tallest heights. Medium porosity windbreakers at the tallest height provide the best drag reduction in a 30º crosswind. Moreover, windbreaks with varying porosities can lead to different levels of wind speed reduction and turbulence intensity, consequently affecting the overall drag experienced by trains [27], [28].

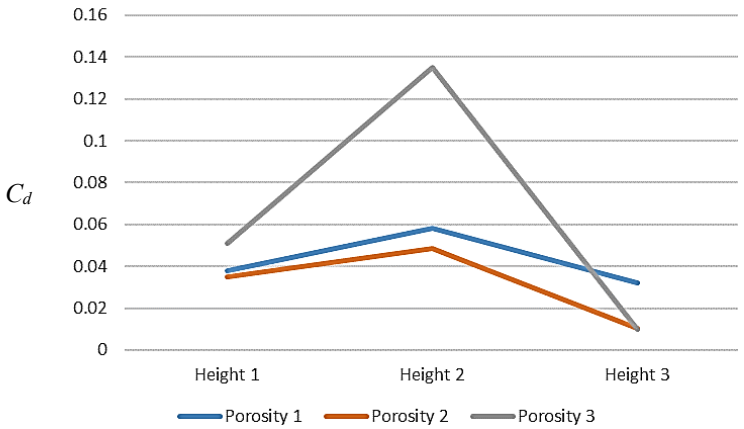

Figure 5. Drag force coefficient (C_d) of high-speed train at 30º crosswind condition

3.2 Drag Force Coefficient at 60º Crosswind Condition

Figure 6 shows the C_d at a 60º crosswind condition. The coefficient of thermal conductivity C_d rises with height for windbreakers with high porosity (50 mm), from 0.3166 at 65 mm to 0.6188 at 195 mm. This indicates that higher windbreakers block more crosswinds and result in increased resistance. On the other hand, the C_d of medium porosity windbreakers (25 mm) decreases significantly with height, from 0.4317 at 65 mm to 0.1068 at 195 mm, suggesting that they efficiently reduce drag by striking a balance between airflow and wind blocking. In the same direction, the taller low-porosity windbreakers (12.5 mm) exhibit a decrease in C_d with height, from 0.4853 at 65 mm to 0.1262 at 195 mm. This means the low-porosity windbreakers reduce drag by blocking more airflow while creating less turbulence.

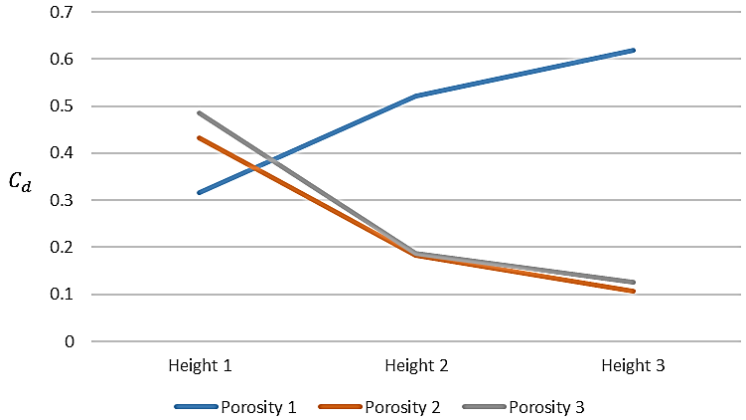

Figure 6. Drag force coefficient (C_d) of high-speed train at 60º crosswind condition

3.3 Side Force Coefficient at 30º Crosswind Condition

The most important factor patterns in aerodynamic performance are revealed by analyzing the side force coefficient (C_s) data for various windbreaker heights and porosities under 30º crosswind conditions, as shown in Figure 7. The highest C_s for high porosity windbreakers (50 mm) is 4.34 at the lowest height (65 mm), suggesting a strong crosswind influence. Effective side force reduction is demonstrated by the considerable reduction to 0.8213 at mid-height (130 mm) and further to 0.3383 at the highest height (195 mm). Similar trends can be seen in medium porosity windbreakers (25 mm), where C_s begins at 4.808 at the lowest height, drops to 1.397 at mid-height, and then rises to 0.7607 at the highest height. Low porosity windbreakers (12.5 mm) have the highest C_s at all heights, starting at 5.132 at the shortest height, reducing to 2.8543 at mid-height, and significantly dropping to 0.9214 at the tallest height.

High porosity windbreakers (4.34) perform better than medium (4.808) and low porosity windbreakers (5.132) in comparison at the smallest height. High porosity (0.8213) performs better than medium (1.397) and low porosity (2.8543) at mid-height. High porosity (0.3383) still outperforms medium (0.7607) and low porosity (0.9214) at the highest height. High porosity windbreakers reduce side forces most effectively overall at all heights, and their efficacy increases with increasing altitude. Low porosity windbreakers are less effective at lower and mid-heights because the airflow is more turbulent due to ground-level obstacles, causing wake effects and deflections that reduce their efficiency. However, at higher altitudes, where the airflow is smoother, these windbreakers effectively block and deflect wind. Medium porosity windbreakers allow some air to pass through, reducing turbulence and vortices. This makes them particularly effective at higher elevations, where they balance wind reduction and airflow control.

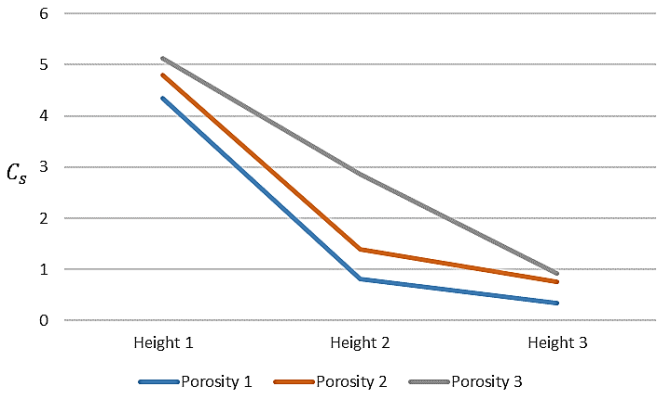

Figure 7. Side force coefficient (C_s) of high-speed train at 30º crosswind condition

3.3 Side Force Coefficient at 60º Crosswind Condition

Considerable patterns are revealed when C_s for windbreakers with different heights and porosities are analyzed in 60º crosswind conditions, as shown in Figure 8. With reference to windbreakers with high porosity (50 mm), C_s is very high at the shortest height (65 mm), indicating significant side forces. However, it significantly decreases at mid-height (130 mm), indicating the best crosswind deflection, and then rises once more at the tallest height (195 mm), although it is still lower than at the shortest height. The medium porosity windbreakers (25 mm) exhibit a poor reduction of side forces, as evidenced by the fact that C_s is maximum at the shortest height. It does, however, decrease at mid-height, staying larger than in windbreakers with high porosity, and efficiently diminishes at the highest height, suggesting enhanced deflection of crosswinds [29].

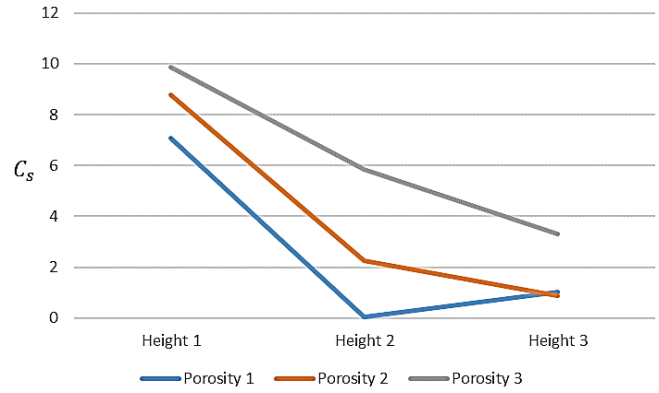

Figure 8. Side force coefficient (C_s) of high-speed train at 60º crosswind condition

Among all porosity levels, the lowest porosity windbreakers (12.5 mm) had the highest C_s at the shortest height, which indicates considerable side forces caused by insufficient airflow passage. Despite decreasing at mid-height, the coefficient of determination is still considerable and remains the highest when compared to windbreakers with high and medium porosity. Conversely, high porosity shows the lowest C_s at the smallest height (65 mm), indicating better performance in reducing side stresses. High porosity is still most effective at mid-height (130 mm), while low porosity results in the largest side forces. Medium porosity has the lowest C_s at the tallest height (195 mm), followed by high porosity. Therefore, medium porosity windbreakers work best at higher heights, whereas high porosity windbreakers work best at shorter and mid-heights to lower C_s at a 60º crosswind.

3.4 Lift Force Coefficient at 30º Crosswind Condition

Assuming 30º crosswind conditions are considered, the lift coefficient (C_l) study reveals varying aerodynamic performance for varying windbreaker heights and porosities. Figure 9 shows the C_l at a 30º crosswind condition. With a little increase at the greatest height (195 mm), high porosity windbreakers (50 mm) exhibit the highest C_l at the shortest height (65 mm) but a significantly lower C_l at mid-height (130 mm), indicating greater lift force reduction. Medium porosity windbreakers (25 mm) provide constant performance, maintaining low C_l values at all heights with a progressive increase from the lowest to the highest heights. The highest C_l at the shortest height is found in low porosity windbreakers (12.5 mm), which subsequently decrease at mid-height and at the tallest height, but remain higher than medium porosity.

In general, windbreakers with high porosity work best at mid-height; those with medium porosity exhibit consistently low C_l at all heights, while those with low porosity increase in effectiveness as height increases but remain less effective at lower heights. Under 30° crosswinds, medium porosity offers the most aerodynamic efficiency.

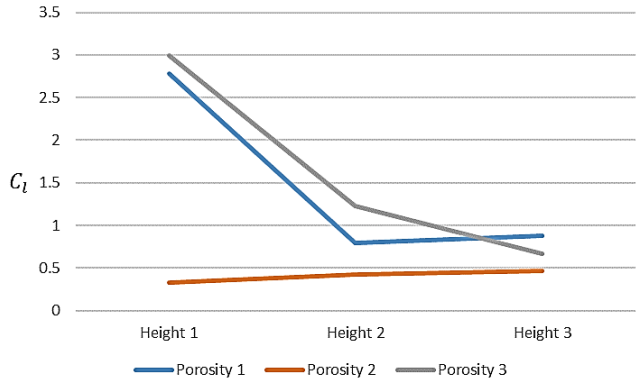

Figure 9. Lift force coefficient (C_l) of high-speed train at 30º crosswind condition

3.5 Lift Force Coefficient at 60º Crosswind Condition

Under 60º crosswind conditions, the C_l for different windbreaker heights and porosities provides significant data about their aerodynamic performance around a 186 mm height train. Figure 10 shows the C_l at 60º crosswind condition, high porosity windbreakers (50 mm) had a high C_l value of 6.258 at the smallest height (65 mm), suggesting substantial lift forces. C_l sharply decreases to 0.0172 at mid-height (130 mm), demonstrating efficient lift force reduction, then climbs slightly to 0.3379 at the greatest height (195 mm). High C_l at the lowest height (6.047) is also observed in medium porosity windbreakers (25 mm). This value decreases to 1.197 at mid-height and to 0.7533 at the highest height, suggesting efficient lift force regulation at higher elevations. With 6.226 at the lowest height, 2.9764 at the mid-height, and 2.4774 at the maximum height, low porosity windbreakers (12.5 mm) have the highest C_l. This indicates that they are less effective in lowering lift forces. All things considered, medium porosity windbreakers and low porosity windbreakers are less effective in minimizing lift forces at all heights than high porosity windbreakers.

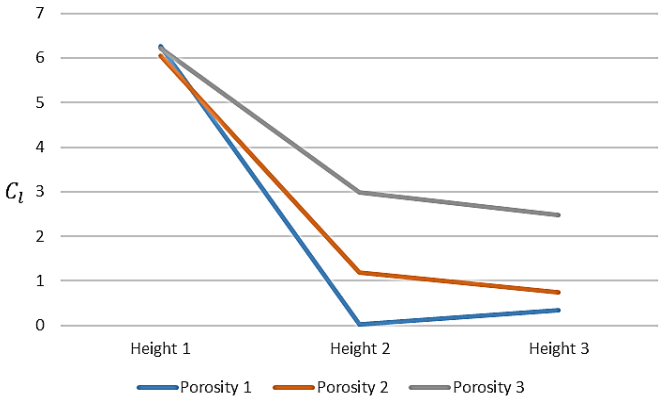

Figure 10. Lift force coefficient (C_l) of high-speed train at 60º crosswind condition

Overall, the high porosity windbreakers are consistently effective at reducing side and lift forces, especially at lower and mid-heights, making them suitable for near-ground installations in areas with moderate terrain-induced turbulence. Medium porosity windbreakers, on the other hand, show excellent performance in drag and lift suppression at greater heights, suggesting their advantage in elevated track sections or viaducts. Low porosity windbreakers exhibit localized effectiveness, particularly at upper levels under high wind incidence, but their performance is generally compromised at lower elevations due to increased turbulence and wake interactions. These insights provide a robust design guideline: optimal aerodynamic load mitigation is achievable through strategic variation of porosity and height along the train's vertical profile, rather than a uniform windbreaker configuration.

3.6 Pressure Contour and Streamlines at 30º Crosswind Condition

To assist with the analysis of pressure changes in fluid flow simulations, a pressure contour visually shows pressure distribution across a surface or inside a fluid domain. The streamline and pressure contour in a 30º crosswind scenario are shown in Figure 11. Effective airflow obstruction and significant wake development with turbulence and circulation zones are indicated by the first row, where a high, low-porosity windbreaker forms a big low-pressure area behind it and a high-pressure zone on its windward side.

Comparisons in the third row show that different windbreaker heights have varied effects. With consistent pressure contours and clean streamlines, the 65 mm windbreaker has little effect on the train due to its strong pressure generation on the windward side and small pressure drop on the lee side. More windward pressure and a more robust low-pressure area on the lee side are produced by the 130 mm windbreaker, strengthening the barrier's effectiveness and increasing aerodynamic effects, turbulence, and wake region length. The biggest effect is from the 195 mm windbreaker, which

creates a wide recirculation zone, a steep pressure gradient, substantial deflection, and turbulence on the lee side. It also causes unusually high windward pressure. The aerodynamic influence on the train rises with windbreaker height, resulting in more chaotic streamline patterns, intricate pressure contours, and interrupted airflow.

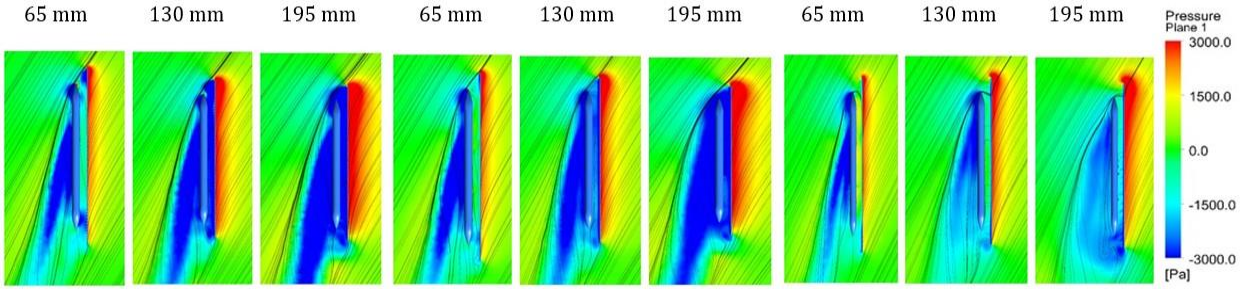

Figure 11. Top view of pressure contour and streamlines at 30º crosswind conditions

3.7 Pressure Contour and Streamlines at 60º Crosswind Condition

The distribution of pressure across a surface is graphically represented by pressure contours, which are often displayed by connecting points of equal pressure using contour plots. With three distinct windbreaker heights and porosities, Figure 12 shows the top view of a train's pressure contour and streamline in a 60º crosswind. Windbreakers with a 50 mm porosity in the first row allow less air to pass through, which smooths the airflow around the train but may also cause pressure to build up. Maximum pressure impact is seen at the highest windbreaker height, which causes airflow streamlines to diverge away from the train.

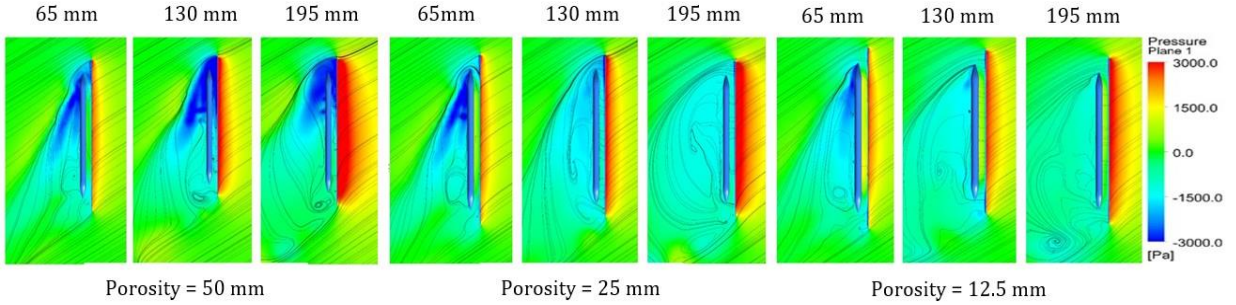

Figure 12. Top view of pressure contour and streamlines 60º crosswind conditions

The windbreakers in the second row have a porosity of 25 mm, which achieves a balance between smoothness and airflow restriction. The pressure impact is maximum at 195 mm height, which causes a large change in the airflow to streamline the following deflection away from the train. Windbreakers with a 12.5 mm porosity that permits strong airflow are seen in the third row. Compared to the higher windbreakers, the 65 mm height windbreaker has less pressure impact and causes less turbulence around the train. In general, larger pressure impacts, more pronounced airflow deflection, and increased turbulence surrounding the train are caused by higher windbreakers and lower porosity [30].

3.8 Surface Pressure Contour at 30º Crosswind Condition

The pressure distribution across surfaces is shown by pressure contours, which are represented by contour lines or colour gradients. This information is key to understanding airflow around trains. These impacts are examined for a train in crosswind conditions with varying porosities and windbreaker heights in Figure 13. Despite having a high porosity, the 65 mm windbreaker provides minimal crosswind resistance, which results in a maximum pressure increase and extremely variable pressure contours on the train. Stronger barriers are provided by the 130 mm and 195 mm windbreakers, which lead to less pressure gradients on the windbreakers and mild pressure differentials on the train, which improve aerodynamic performance.

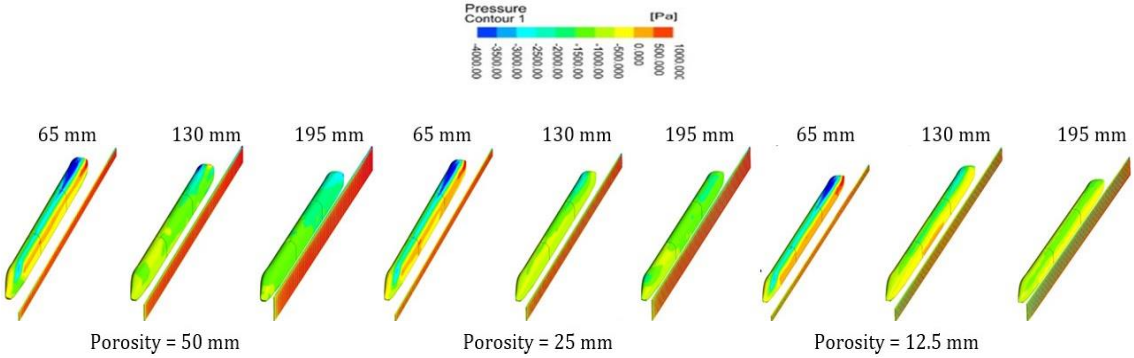

Figure 13. Isometric view pressure contour at 30º crosswind condition

The 65 mm windbreaker displays considerable pressure increases and different train impacts in a 30º crosswind. Greater crosswind blocking is achieved by taller windbreakers (195 and 130 mm), which provide average pressure gradients on the windbreakers and moderate rises along the train. The 130 mm and 195 mm windbreakers have less of an effect on pressure changes on the train than the 65 mm windbreaker, which has 12.5 mm porosity.

3.9 Surface Pressure Contour at 60º Crosswind Condition

The pressure contours caused by crosswinds on windbreakers and a train are shown in Figure 14. While the train encounters various impacts in each situation, the pressure contours on the windbreaker remain constant. With a 50 mm porosity windbreaker, there is maximum pressure impact at the midway height of the train due to the low windbreaker experiencing significant pressure. This happens as a result of the windbreaker being forced around and colliding with the train due to the significant porosity's restriction of airflow. The impact of pressure on the train is less evident at the other two windbreaker heights.

The low windbreaker demonstrates a major pressure influence on the windbreaker and train, with a porosity of 25 mm. Because of the greater porosity, more airflow flows through and hits the middle to bottom regions of the train, suggesting a larger pressure impact [31]. Less impact is shown by the other windbreakers. More airflow is permitted by the 12.5 mm porosity windbreaker, which has the greatest pressure influence on the train, particularly at the lowest height. The pressure is greatest on the train's bottom side, with slightly less noticeable pressure effects being present at the other two windbreaker heights. Lower porosity and height increase pressure impact on the train, with airflow largely deflecting around less permeable windbreakers.

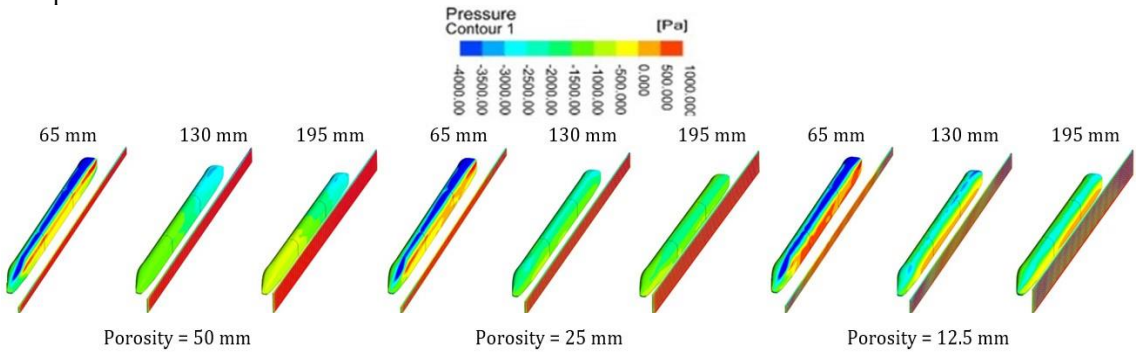

Figure 14. Isometric view pressure contour at 60º crosswind condition

The results from pressure contour and streamline analyses clearly demonstrate that windbreaker design, specifically height and porosity, critically determines the aerodynamic behavior of trains under crosswind conditions. While taller, low-porosity windbreakers effectively shield the train and mitigate pressure variations, they can also induce strong turbulence in the wake.

3.10 Velocity Streamlines at 30º Crosswind Condition

Velocity streamline patterns in Figure 15 show how windbreakers affect a train that is 186 mm tall in a 30º crosswind. Because the 65 mm windbreaker is much lower than the train, airflow can mostly travel over it with little deviation. Because of the unhindered airflow, this causes a direct crosswind impact on the upper portion of the train, creating turbulence and vortices behind it. A 130 mm windbreaker directs airflow upward and along the sides of the train while covering a larger portion of the train's height. In contrast to the 65 mm windbreaker, this deflects the crosswind away from the bottom and central sections of the train, reattaching streamlines higher up and decreasing turbulence.

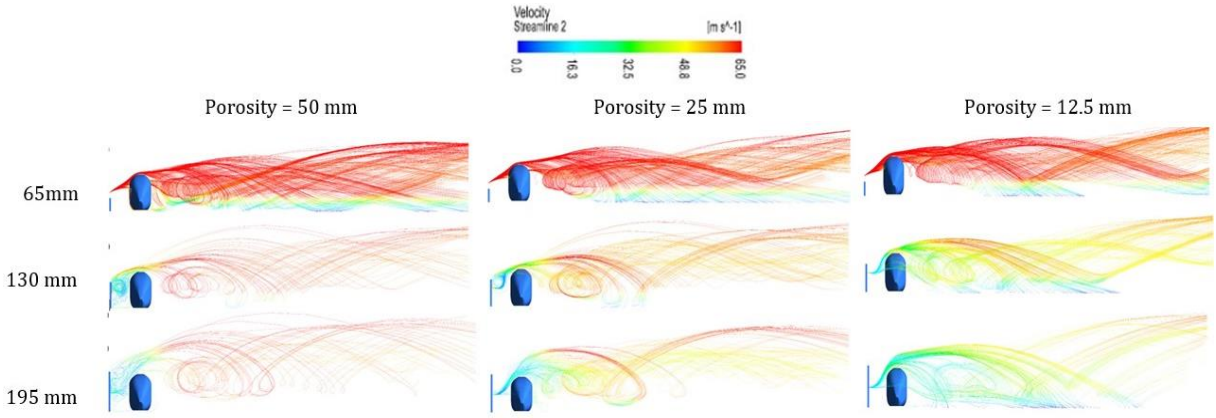

Figure 15. Velocity streamlines at 30º crosswind condition

The 195 mm windbreaker, on the other hand, is higher than the train and blocks airflow as well as deflects streamlines well above the train. This whole barrier increases turbulence because of its high porosity, but reduces crosswind impact over the entire train height. The windbreaker's airflow passage is impacted by porosity variations of 50 mm, 25 mm, and 12.5 mm, which in turn affect the turbulence levels behind the windbreaker and train. Lower porosity improves the train's overall aerodynamic efficiency at all windbreaker heights by lowering turbulent flow and stabilizing pressure differentials.

3.11 Velocity Streamlines at 60º Crosswind Condition

The correlation between airflow and windbreakers at different heights is shown in Figure 16 through velocity streamline analysis. The windbreaker with the highest velocity, which hits the train directly, is the 65 mm height windbreaker for windbreakers with 50 mm porosity. This is because the airflow passes over it with minimal impediment. At 130 mm and 195 mm heights, high porosity prevents airflow through the windbreaker, creating turbulence and circulation behind it before the air is deflected around the train, resulting in smoother, streamlined velocity.

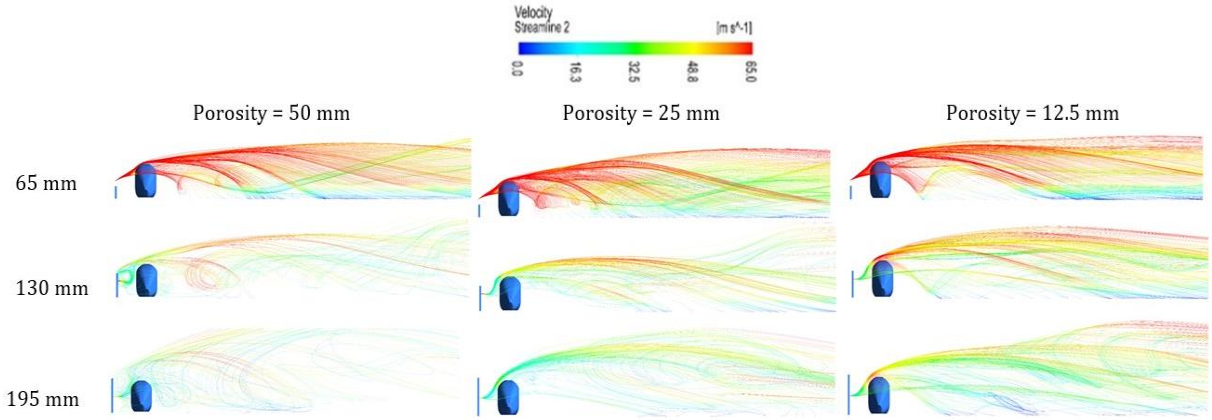

Figure 16. Velocity streamlines at 60º crosswind condition

Velocity streamlines appear constant and smooth at all windbreaker heights with 25 mm porosity. With no airflow hindrance, the 65 mm height windbreaker reaches its maximum velocity and hits the train directly. Because there is less porosity at heights of 130 mm and 195 mm, airflow flows through more easily, minimizing turbulence and maintaining stable conditions for the train. Thus, windbreakers with reduced porosity permit more fluid airflow, reducing turbulence and guaranteeing constant velocity conditions surrounding the train at different elevations.

4. CONCLUSION

This study analyzed the impact of windbreaker height and porosity on the aerodynamic performance of high-speed trains subjected to 30º and 60º crosswinds. The results demonstrate that optimizing windbreaker designs based on wind conditions significantly enhances aerodynamic efficiency. For 30º crosswinds, shorter windbreakers (65 mm) with medium porosity (25 mm) effectively minimize drag. Medium-height windbreakers (130 mm) with medium porosity also perform well under 30º crosswinds. In contrast, for 60º crosswinds, taller windbreakers (195 mm) benefit the most from medium and low porosity designs. Medium porosity windbreakers (25 mm) consistently reduce drag, side force, and lift force coefficients across all configurations. Low porosity (12.5 mm) often obstructs airflow, increasing drag and side forces, especially for shorter windbreakers. Meanwhile, high porosity (50 mm) windbreakers effectively reduce side forces at medium and tall heights. These findings emphasize the need for customized windbreaker layouts to mitigate crosswind effects and improve aerodynamic performance.

To enhance future research and practical application, several recommendations are proposed. Expanding the range of porosity levels and windbreaker heights can help identify optimal designs for various crosswind conditions. Incorporating dynamic crosswind angles instead of fixed values would better reflect real-world variability. Advanced turbulence models, such as Large Eddy Simulation (LES) or Detached Eddy Simulation (DES), should be employed to represent unsteady flow features more effectively. Additionally, validating CFD results through wind tunnel and real-world testing is essential to ensure practical applicability.

ACKNOWLEDGEMENT

This research was supported by the Malaysia Ministry of Higher Education (MOHE) through the Fundamental Research Grant Scheme (FRGS/1/2020/TK02/UTHM/03/4).

CONFLICT OF INTEREST

The authors declare that there is no conflict of interest.

AUTHORS' CONTRIBUTION

N. A. Norhelmi: Conceptualization, Methodology, Software, Formal analysis, Data Curation, Visualization, Original Draft Preparation

I. A. Ishak: Supervision, Project Administration, Funding Acquisition, Review and Editing

M. Arafat: Methodology, Visualization, Review and Editing.

N. M. Maruai: Investigation, Data Curation.

N. H. Shaharuddin: Project Administration, Funding Acquisition.

N. A. Samiran: Funding Acquisition, Resources.

N. Darlis: Validation, Formal Analysis.

R. A. Jalil: Supervision, Conceptualization.

REFERENCES

[1] I. A. Ishak, M. S. Mat Ali, M. F. Mohd Yakub, and S. A. Z. Shaikh Salim, "Effect of crosswinds on aerodynamic characteristics around a generic train model," *International Journal of Rail Transportation*, vol. 7, no. 1, pp. 1–32, 2018.

[2] I. A. Ishak, N. Maruai, F. M. Sakri, N. A. S. Rahmah Mahmudin, S. Sulaiman, S. F. Z. Abidin, et al., "Numerical analysis on the crosswind influence around a generic train moving on different bridge configurations," *Journal of Advanced Research in Fluid Mechanics and Thermal Sciences*, vol. 89, no. 1, pp. 76–98, 2017.

[3] H. Tian, "Formation mechanism of aerodynamic drag of high-speed train and some reduction measures," *Journal of Central South University of Technology*, vol. 16, no. 1, pp. 166–171, 2009.

[4] Z. Sun, H. Dai, H. Hemida, T. Li, and C. Huang, "Safety of high-speed train passing by windbreak breach with different sizes," *Vehicle System Dynamics*, vol. 58, no. 12, pp. 1935–1952, 2020.

[5] S. A. Hashmi, H. Hemida, and D. Soper, "Wind tunnel testing on a train model subjected to crosswinds with different windbreak walls," *Journal of Wind Engineering and Industrial Aerodynamics*, vol. 195, p. 104013, 2019.

[6] J. Niu, D. Zhou, and X. Liang, "Numerical investigation of the aerodynamic characteristics of high-speed trains of different lengths under crosswind with or without windbreaks," *Engineering Applications of Computational Fluid Mechanics*, vol. 12, no. 1, pp. 195–215, 2018.

[7] I. A. Ishak, M. S. M Ali, F. M. Sakri, F. H. Zulkifli, N. Darlis, R. Mahmudin, et al., "Aerodynamic characteristics around a generic train moving on different embankments under the influence of crosswind," *Journal of Advanced Research in Fluid Mechanics and Thermal Sciences*, vol. 61, no. 1, pp. 106–128, 2019.

[8] T. Liu, Z. Chen, X. Zhou, and J. Zhang, "A CFD analysis of the aerodynamics of a highspeed train passing through a windbreak transition under crosswind," *Engineering Applications of Computational Fluid Mechanics*, vol. 12, no. 1, pp. 137–151, 2018.

[9] M. Wang, Z. Wang, X. Qiu, X. Li, and X. Li, "Windproof performance of wind barrier on the aerodynamic characteristics of high-speed train running on a simple supported bridge," *Journal of Wind Engineering and Industrial Aerodynamics*, vol. 223, p. 104950, 2022.

[10] G. M. Heisler and D. R. Dewalle, "Effects of Windbreak Structure on Wind Flow," in *Windbreak Technology*, Elsevier, 1988, pp. 41–69.

[11] B. Blocken, T. Stathopoulos, and J. Carmeliet, "Wind environmental conditions in passages between two long narrow perpendicular buildings," *Journal of Aerospace Engineering*, vol. 21, no. 4, pp. 280–287, 2008.

[12] X. Dong, T. Liu, Y. Xia, F. Yang, Z. Chen, and Z. Guo, "Comparative analysis of the aerodynamic performance of trains and dynamic responses of catenaries for windbreak walls with different heights under crosswind," *Proceedings of the Institution of Mechanical Engineers, Part F: Journal of Rail and Rapid Transit*, vol. 237, no. 3, pp. 335–346, 2023.

[13] J. Niu, Y. Zhang, R. Li, Z. Chen, H. Yao, and Y. Wang, "Aerodynamic simulation of effects of one- and two-side windbreak walls on a moving train running on a double track railway line subjected to strong crosswind," *Journal of Wind Engineering and Industrial Aerodynamics*, vol. 221, p. 104912, 2022.

[14] M. Mohebbi, Y. Ma, and R. Mohebbi, "The influence of inclined barriers on airflow over a high speed train under crosswind condition," in *New Research on Railway Engineering and Transportation*, IntechOpen, 2023.

[15] Z. Sun, H. Dai, H. Gao, T. Li, and C. Song, "Dynamic performance of high-speed train passing windbreak breach under unsteady crosswind," *Vehicle System Dynamics*, vol. 57, no. 3, pp. 408–424, 2019.

[16] M. Mohebbi and M. A. Rezvani, "Two-dimensional analysis of the influence of windbreaks on airflow over a high-speed train under crosswind using lattice Boltzmann method," *Proceedings of the Institution of Mechanical Engineers, Part F: Journal of Rail and Rapid Transit*, vol. 232, no. 3, pp. 863–872, 2018.

[17] M. Arafat, I. A. Ishak, and N. Mohd Maruai, "Numerical analysis of sudden wind load impact on aerodynamic performance in next-generation high-speed trains," *Iranian Journal of Science and Technology, Transactions of Mechanical Engineering*, vol. 49, no. 1, pp. 517–532, 2025.

[18] M. Arafat, S. Rajendran, I. A. Ishak, M. Al, and A. M. Zin, "Effects of crosswinds on the flow structure around a next-generation high-speed train exiting a tunnel," *Jurnal Teknologi (Sciences & Engineering)*, vol. 86, no. 6, pp. 29–37, 2024.

[19] J. Zhang, A. Adamu, F. Gidado, M. Tang, O. Ozer, and X. Chen, "Flow control for aerodynamic drag reduction of a high-speed train with diversion slots on bogie regions," *Physics of Fluids*, vol. 35, no. 11, p. 115111, 2023.

[20] X.-S. Huo, T.-H. Liu, Z.-W. Chen, W.-H. Li, J.-Q. Niu, and H.-R. Gao, "Aerodynamic characteristics of double-connected train groups composed of different kinds of high-speed trains under crosswinds: A comparison study," *Alexandria Engineering Journal*, vol. 64, pp. 465–481, 2023.

[21] A. Narjisse and K. Abdellatif, "Assessment of RANS turbulence closure models for predicting airflow in neutral ABL over hilly terrain," *International Review of Applied Sciences and Engineering*, vol. 12, no. 3, pp. 238–256, 2021.

[22] X. Xiong, R. Cong, X. Li, Y. Geng, M. Tang, S. Zhou, et al., "Unsteady slipstream of a train passing through a high-speed railway tunnel with a cave," *Transportation Safety and Environment*, vol. 4, no. 4, p. tdac032, 2022.

[23] X. Xu, H. Li, and Y. Lin, "Mesh-order independence in CFD simulation," *IEEE Access*, vol. 7, pp. 119069–119081, 2019.

[24] I. A. Ishak, M. S. Mat Ali, and S. A. Z. ShaikhSalim, "Mesh size refining for a simulation of flow around a generic train model," *Wind and Structures*, vol. 29, no. 3, pp. 223-247, 2017.

[25] R. Timsina and Z. Barahmand, "Mesh Sensitivity Analysis of an Entrained Flow Biomass Gasifier: A CPFD Study," in *Proceedings of the 63rd International Conference of Scandinavian Simulation Society, SIMS 2022, Trondheim, Norway, September 20-21, 2022*, Oct. 2022, pp. 371–377.

[26] M. Fragner, K. A. Weinman, R. Deiterding, U. Fey, and C. Wagner, "Comparison of industrial and scientific CFD approaches for predicting cross wind stability of the NGT2 model train geometry," *The International Journal of Railway Technology*, vol. 4, no. 1, pp. 1–28, 2015.

[27] J. P. Bitog, I. B. Lee, H. S. Hwang, M. H. Shin, S. W. Hong, I. H. Seo, et al., "A wind tunnel study on aerodynamic porosity and windbreak drag," *Forest Science and Technology*, vol. 7, no. 1, pp. 8–16, 2011.

[28] A. E. Loeffler, A. M. Gordon, and T. J. Gillespie, "Optical porosity and windspeed reduction by coniferous windbreaks in Southern Ontario," *Agroforestry Systems*, vol. 17, no. 2, pp. 119–133, 1992.

[29] D. Zhang, H. Gao, W. Jiang, X. Dong, J. Song, and G. Hu, "Mitigating crosswind response of a high-speed train passing the end of windbreak walls," *Advances in Wind Engineering*, vol. 1, no. 1, p. 100009, 2024.

[30] I. Koh, C. R. Park, W. Kang, and D. Lee, "Seasonal effectiveness of a korean traditional deciduous windbreak in reducing wind speed," *Journal of Ecology and Environment*, vol. 37, no. 2, pp. 91–97, 2014.

[31] J. Kucera, J. Podhrázská, P. Karásek, and V. Papaj, "The effect of windbreak parameters on the wind erosion risk assessment in agricultural landscape," *Journal of Ecological Engineering*, vol. 21, no. 2, pp. 150–156, 2020.